ON

DEEP INELASTIC ν SCATTERING

B C Barish

California Institute of Technology

INTRODUCTION

Papers on deep inelastic neutrino scattering were submitted by three groups: Gargamelle - CERN (papers 511, 512 and 513), Harvard-Pennsylvania-Wisconsin-Fermilab (691 and 694) and Caltech-Fermilab (586 and 588). New information on normalized cross-sections at high energy, distributions in the scaling variables $x = Q^2/2ME_h$ and $y = E_h/E_o$, and tests of scaling in the Q^2 distributions were presented. The Gargamelle-CERN group also gave new tests of certain sum rules. The following are short summaries of the talks given on the results of these three groups by M Haguenauer (Ecole Polytechnique) on the CERN experiment, R Imlay (U of Wisconsin) and F Sciulli (Caltech) on the two Fermilab experiments.

"GARGAMELLE" EXPERIMENT

(Aachen, Brussels, CERN, Ecole Polytechnique Paris, Milano, Orsay, University College London)

Presented by M Haguenauer

We present here further studies of charged-current neutrino interactions in the heavy liquid bubble chamber Gargamelle (freon CF_3Br filling) exposed to a focussed wideband beam at the CERN PS [1]. It was previously observed that both $\sigma(\nu)$ and $\sigma(\bar{\nu})$ as well as the mean values of q^2 increase linearly with energy over the range E = 1 - 10 GeV. Furthermore the ratio $\sigma(\bar{\nu})/\sigma(\nu)$ was found to be independent of energy and have a mean value of 0.38 ± 0.02 [2].

I. TOTAL AND PARTIAL CROSS-SECTIONS

a) Neutrino total cross-section

Using the measured flux the ν_μ cross-section has now been determined for energies up to 20 GeV. Fig. 1 shows that it is compatible with a linear increase and a straight line fit over the whole range gives

$\sigma^\nu = (0.76 \pm 0.02)\ E\ 10^{-38}\ cm^2$, with E in GeV, in agreement with the published result.

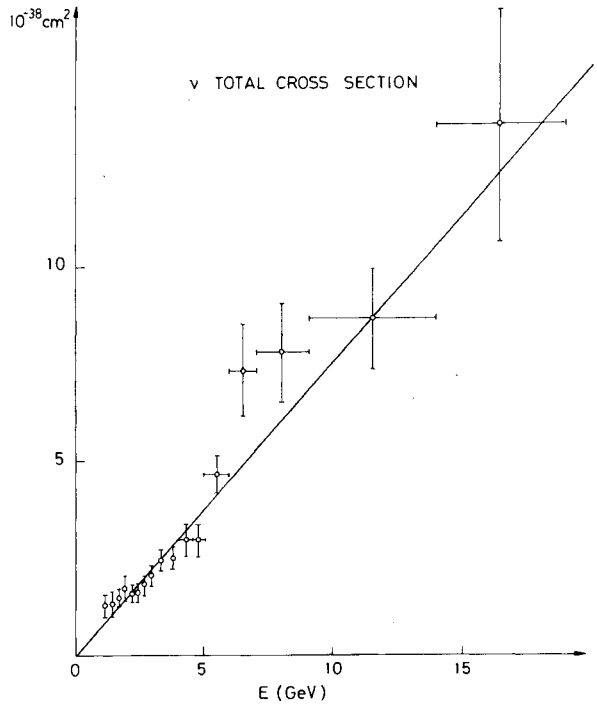

Fig. 1 Linear increase of the total neutrino cross section with energy.

At E less than 5 GeV the ν_μ come predominantly from pion decay, whereas at E larger than 8 GeV they come from kaon decay. Straight line fits in these two regions give:

$E < 5$ GeV $\quad \sigma^\nu = (0.74 \pm 0.03)\ E\ 10^{-38}\ cm^2$

$E > 8$ GeV $\quad \sigma^\nu = (0.77 \pm 0.10)\ E\ 10^{-38}\ cm^2$

So we cannot see any difference in total cross-section between neutrinos from pions and neutrinos from kaons.

The above errors do not include a ±6% error on the flux normalization.

b) Strange particle production

For this study we analysed 200,000 pictures. In order to assure good efficiencies we searched only for the charged decays of K^o, $\bar{K}^o$ and Λ^o and for K^+ decays at rest. The numbers of events are indicated below.

1. Associated production

		Observed
$K\bar{K}$	K^+K^-	undetectable
	K^+K^o	0
	K^oK^-	undetectable
$K\Upsilon$	$K^+\Lambda^o$	10
	$K^+\Sigma^{+,o,-}$	undetectable
	$K^o\Lambda^o$	2
	$K^o\Sigma^{+,o,-}$	undetectable

in addition we observed 27 single Λ^o's (from $K^+\Lambda^o$ and $K^o\Lambda^o$, K not observed).

2. $\Delta S = 1$ production

		Observed
K	K^+	16
	K^o	10

Only certain channels were detectable. Consequently we can only give a lower limit for associated production normalized to the total charged current cross-section

$$\frac{\sigma_{\text{ass. prod.}}}{\sigma_{\text{total}}} > 0.5\% \quad \text{at} \quad > 90\%\ \text{CL.}$$

and an upper limit for $\Delta S = 1$ production

$$\frac{\sigma_{\Delta S = 1}}{\sigma_{\text{total}}} < 2\% \quad \text{at} > \quad 90\%\ \text{CL.}$$

II. DIFFERENTIAL CROSS-SECTIONS AND STRUCTURE FUNCTIONS

In the deep inelastic scaling region the double differential cross-section has the form:

$$\frac{d^2\sigma^{\nu,\bar{\nu}}}{dx\,dy} = \frac{G^2 ME}{\pi}\left\{(1 - y + \frac{y^2}{2})\ F_2(x) \pm y(1 - \frac{y}{2})\ x\ F_3(x)\right\} \qquad (1)$$

assuming the CALLAN-GROSS relation $F_2(x) = 2xF_1(x)$

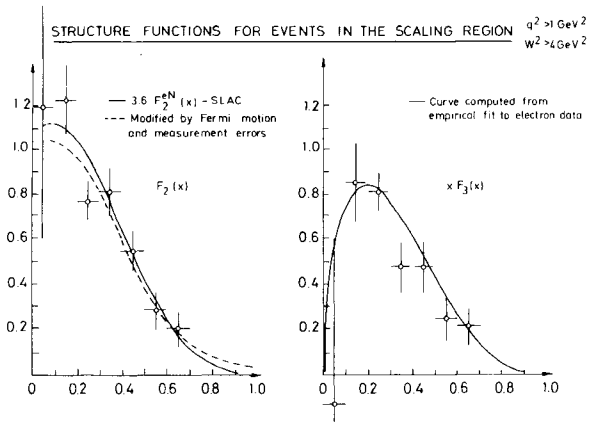

Fig. 2 $F_2(x)$ and $xF_3(x)$ in the scaling region derived from the sum and difference of neutrino cross section. $F_2(x)$ is compared with predictions from the SLAC data assuming the fractionally charged quark-parton model.

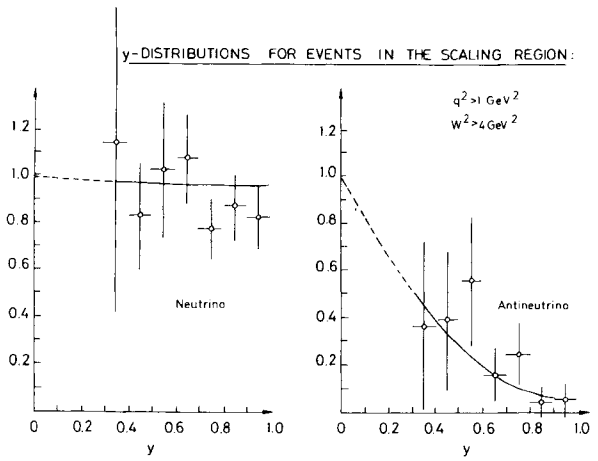

Fig. 3 Neutrino and antineutrino y - distributions in the scaling region.

a) Events in the scaling region

The SLAC-MIT data have shown that scaling occurs in the region $q^2 > 1$ GeV^2 and $W^2 > 4$ GeV^2. Fig. 2 shows $F_2(x)$ and $xF_3(x)$ assuming (1) integrated over y. We see that both agree in shape as well as in magnitude with an empirical fit to the SLAC data [3] multiplied by a factor of 3.6 due to the quark model. The y distributions (Fig. 3) are compatible with the scaling hypothesis.

b) Distributions without scaling cuts

To describe the events without cuts we used the BLOOM-GILMAN variable [4] $x' = q^2/(2M\nu + M^2)$ where ν is the energy transferred and M the nucleon mass. This variable has several advantages:

- the SLAC-MIT data have shown that scaling occurs earlier in x' than in x.
- elastic events are treated on the same footing as the others.
- the errors are much more smaller in x' than in x.

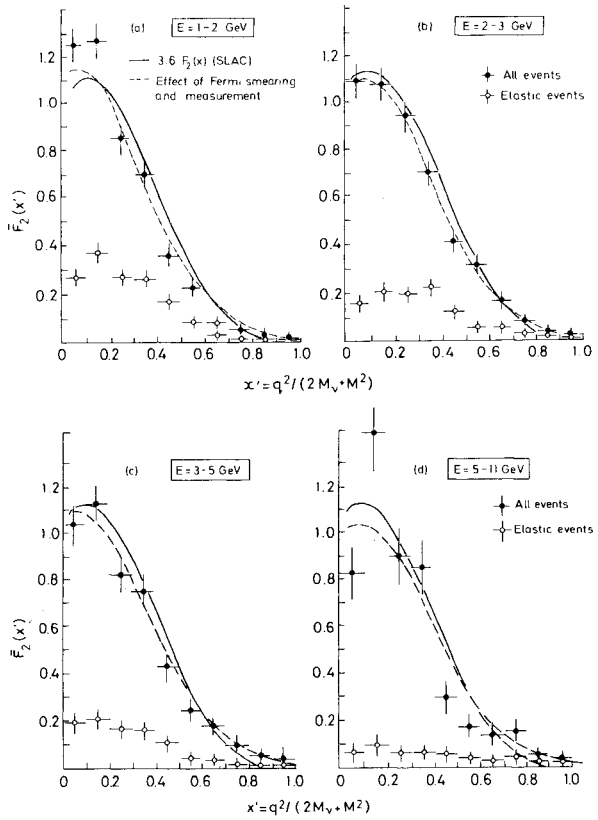

Fig. 4 Distribution in $\bar{F}_2(x')$ for various energy bins with no cuts applied to q^2 and W^2.

In what follows we shall assume that x can be replaced by x' everywhere in the scaling formula (1) and we define the corresponding new structure functions $\bar{F}_1(x')$, $\bar{F}_2(x')$ and $\bar{F}_3(x')$ is plotted in Fig. 4 for several bins of energy and we can see that within 10 to 20% errors the shape and magnitude is independent of energy and it agrees very well with the electroproduction result.

c) The y distributions

Until we find a y' variable which describes the experimental distributions as well as x', we can only give qualitative results. At small energies the distributions are dominated by the elastic channel, but as the energy grows the distributions approach those expected by scaling.

III. SUMRULES

a) The GROSS-LLEWELLYN SMITH sumrule [5]

For a nucleon target of B = Y = 1 composed of GELLMANN-ZWEIG quarks the GLS sumrule has the form:

$$\frac{1}{2}\int (F_3^{\nu n} + F_3^{\nu P})dx = 3(1 - \frac{1}{2}\sin^2\theta_c)$$

Taking into account the neutron/proton ratio (1.19 in CF_3Br), we expect

$$\left(\int F_3^{\nu N}\, dx\right)_{freon} = 3.1$$

If we assume that experimentally

- x may be replaced by x'
- $\bar{F}_3(x')$ is well behaved at the origin,

then we can calculate $\int F_3^{\nu N}(x)dx$ (Fig. 6). We see that this integral is rather constant with energy. For the mean value we find:

$$\int_0^1 \bar{F}_3\,(x')dx' = 3.2 \pm 0.6$$

b) The ADLER sumrule

The so called β sumrule of ADLER [6] is a fixed $-q^2$, infinite-energy sumrule. For a target of

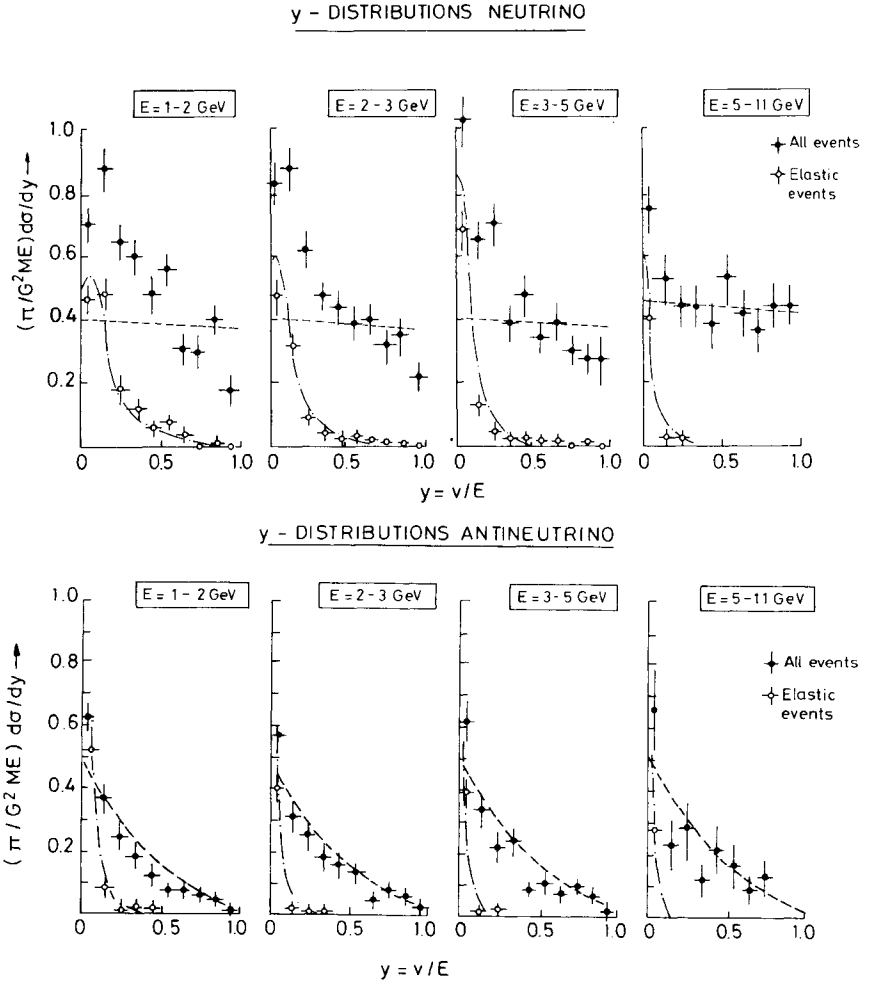

Fig. 5 Distribution in y for neutrino and antineutrino and for various energy bins, showing an approach to the scaling distributions as the energy grows.

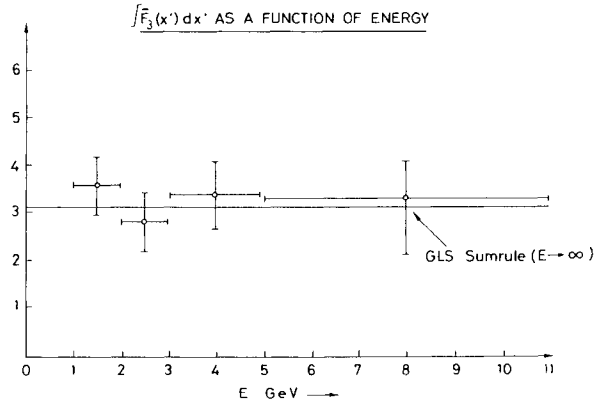

Fig. 6 Evaluation of the Gross-Llewellyn-Smith sum rule as a function of energy.

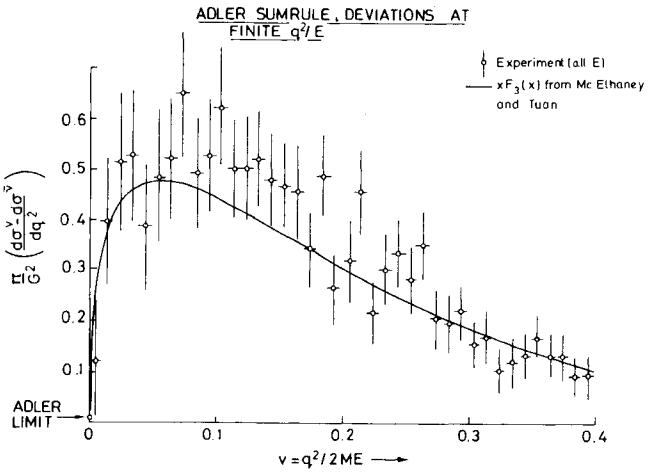

Fig. 7 Variation with $q^2/2ME$ of the difference between neutrino and antineutrino cross sections showing that convergence to the Adler limit occurs only at very small values.

isospin component I_3 and hypercharge Y, it has the form:

$$\lim_{E\to\infty} \left(\frac{d\sigma^{\nu} - d\sigma^{\bar{\nu}}}{dq^2}\right) = -\frac{G^2}{\pi}\left\{2I_3 \cos^2\theta_c + \frac{2I_3+Y}{2}\sin^2\theta_c\right\}$$

For a freon target, it would give

$$\lim_{E\to\infty} \left(\frac{d\sigma^{\nu} - d\sigma^{\bar{\nu}}}{dq^2}\right) = 0.01\ \frac{G^2}{\pi}$$

In order to investigate in our low energy region, we plot our data as a function of the quantity $\nu = q^2/2ME$ (Fig. 7). The full line has been computed using an empirical fit for $F_3(x)$ from the SLAC data and the ADLER sumrule discussed in terms of scaling. We see that convergence occurs only at very small values of $q^2/2ME$, and at $q^2 \sim 0$ we find:

$$\left(\frac{d\sigma^{\nu} - d\sigma^{\bar{\nu}}}{dq^2}\right)_{\text{observed}} - \left(\frac{d\sigma^{\nu} - d\sigma^{\bar{\nu}}}{dq^2}\right)_{\text{Adler}} < 0.3\ G^2/\pi$$

IV. TEST FOR THE QUARK-PARTON MODEL, RATIO OF π^+/π^-

As stated by FEYNMAN [7] we can define the parton fragmentation functions $D_\alpha^{\pi^+}(z)$ and $D_\alpha^{\pi^-}(z)$ with $\alpha = u, d, \bar{u}, \bar{d}$ (we neglect s and $\bar{s}$) and with z = (energy of the pion)/(total energy of the hadrons). Neutrinos interact only with d and $\bar{u}$ quarks, while $\bar{\nu}$ interact only with u and $\bar{d}$.

So for example for νp we can write (with the notation of Ref. 7):

$$D^{\pi^+}(x, z) = d(x)\, D_d^{\pi^+}(z) + \frac{1}{3}\,\bar{u}(x)\, D_{\bar{u}}^{\pi^+}(z)$$

and $$D^{\pi^-}(x, z) = d(x)\, D_d^{\pi^+}(z) + \frac{1}{3}\,\bar{u}(x)\, D_{\bar{u}}^{\pi^-}(z)$$

By charge conjugation the probability of a d yielding a π^+ is the same for $\bar{u}$ producing a π^+, therefore:

$$\frac{D^{\pi^+}(x, z)}{D^{\pi^-}(x, z)} = \frac{Dd^{\pi^+}(z)}{D_d^{\pi^-}(z)} = A(z)$$

The same holds for νn and also for $\bar{\nu}$p and $\bar{\nu}$n. Assuming charge symmetry:

$$\left(\frac{D^{\pi^+}(x, z)}{D^{\pi^-}(x, z)}\right)_{\nu} = \left(\frac{D^{\pi^-}(x, z)}{D^{\pi^+}(x, z)}\right)_{\bar{\nu}} = A(z)$$

and this ratio would be independent of x for any z region. The experimental results are plotted in Figs. 8 and 9. We see that they agree very well. The dashed curve corresponds to a calculation due to ALBRIGHT and CLEYMANS using the SLAC results [8].

(see over)

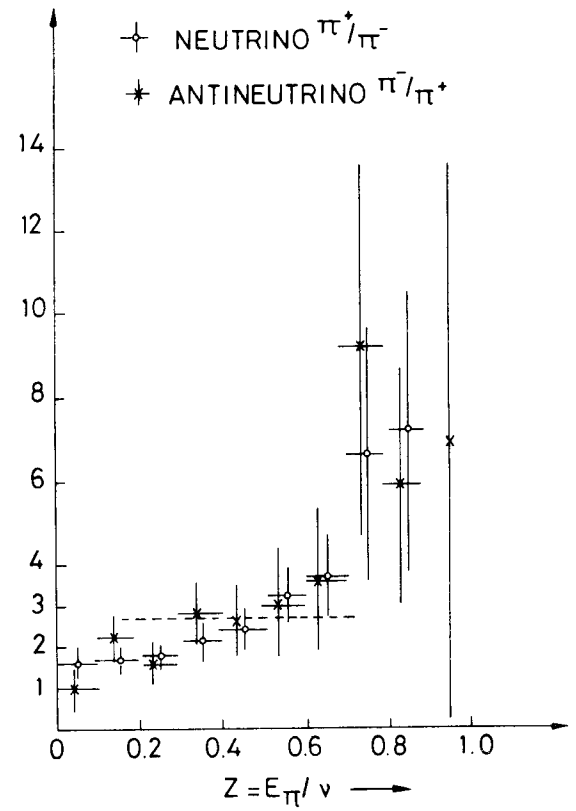

Fig. 8 Current fragmentation charge ratios for neutrino and antineutrino.

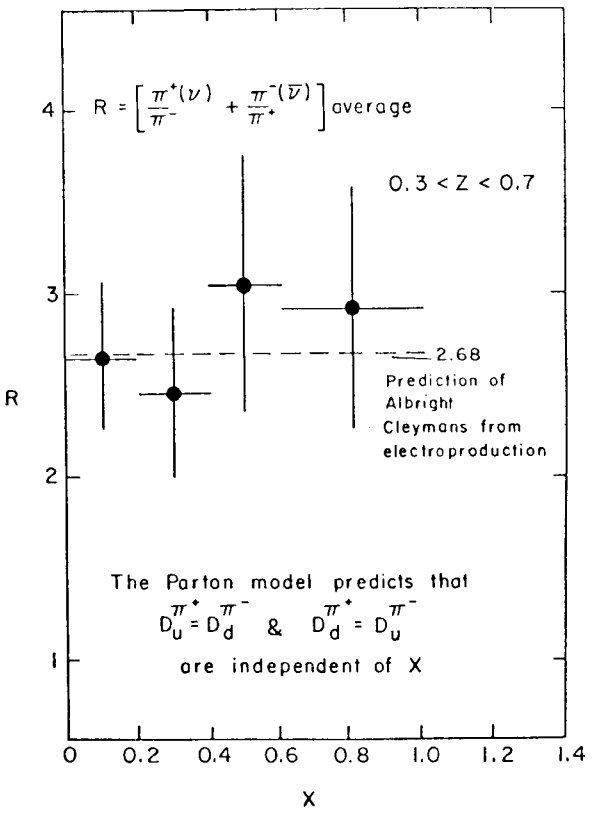

Fig. 9 Mean current fragmentation charge ratio plotted versus x.

REFERENCES

1. Th. Eichten et al, PL 40B No 5 (1972) 593.
2. Th. Eichten et al, PL 46B No 2 (1973) 274.
3. A. Bodek et al, PRL 30 (1973) 1087; A. Bodek, M.I.T. thesis (1973); R. McElhaney and S.F. Tuan PR D8 (1973) 2267; J.T. Dakin and G.J. Feldman, PR D8 (1973) 2862.
4. E. Bloom and F. Gilman, PRL 25 (1970)1140.
5. D.J. Gross and C.H. Llewellyn-Smith, NP B14 (1969) 337.
6. S.L. Adler, PR 143 (1966) 1144.
7. R.P. Feynman in Photon and Hadron Interactions (1972) published by W.A. Benjamin.
8. C.H. Albright and J. Cleymans, CERN TH 1829.

HARVARD-PENNSYLVANIA-WISCONSIN-FERMILAB NEUTRINO EXPERIMENT

R Imlay

University of Wisconsin

Data have been obtained in an experimental study of neutrino interactions at the Fermi National Accelerator Laboratory. The experimental method has been described earlier.[1,2] An enriched beam of neutrinos or antineutrinos impinged on a pure liquid scintillator ionization calorimeter in which the neutrino-nucleon interaction occurred, and in which the hadron energy E_h was measured. The vector momentum of the emerging muon P_μ was measured in a magnetic spectrometer directly downstream of the target-detector. The neutrino energy E_ν was computed from the sum $E_\nu = E_h + E_\mu$. The calorimeter and muon spectrometer were calibrated with pions and muons of known energy between 15 - 150 GeV. The resolution functions so obtained were included in the calculations of the expected distributions.

TOTAL CROSS SECTIONS

We address three aspects of these data:

1) the value of α^ν, the slope of the total neutrino cross-section vs energy obtained by a flux independent method which uses quasielastic events for normalization

2) The relative energy dependence of the neutrino and anti-neutrino cross section and

3) the value of $\bar{\alpha}^\nu/\alpha^\nu$ obtained in a flux independent manner.

We note that the bulk of the neutrino and antineutrino interactions occur on C^{12} which is an I = 0 nucleus for which Glauber shielding corrections are expected to be

small. The quasielastic process $\nu_\mu + n \to \mu^- + p$ and Δ production $\nu_\mu + p \to \Delta^{++} + \mu^-$ are expected to have two interesting properties:

1) the cross sections become energy independent at high energy and

2) the cross sections for neutrino and antineutrino scattering become equal at high energy.

These properties have been directly verified [3] at lower energies and form the basis for our method to measure absolute cross sections. Because of the excellent energy response of a large liquid scintillation detector to low energy hadrons, quasielastic and Δ production events are directly detected. The invariant mass (W) distribution is shown in Fig 1a combining neutrinos and antineutrinos. Figures 1b and 1c show the same distribution for events with $Q^2 < 1$ and $Q^2 < 0.5$ $(GeV/c)^2$, respectively. A clustering of events at low W centered on the N and Δ mass is observed. The continuum contribution at higher W is observed to diminish as Q^2 is reduced as expected for deep inelastic scattering thus reducing the background under the quasielastic and Δ production events. Below a Q^2 of 0.6 GeV^2, the continuum background is small, and the shape of $\frac{d\sigma}{dQ^2}$ is in good agreement with low energy quasi-elastic scattering data[3].

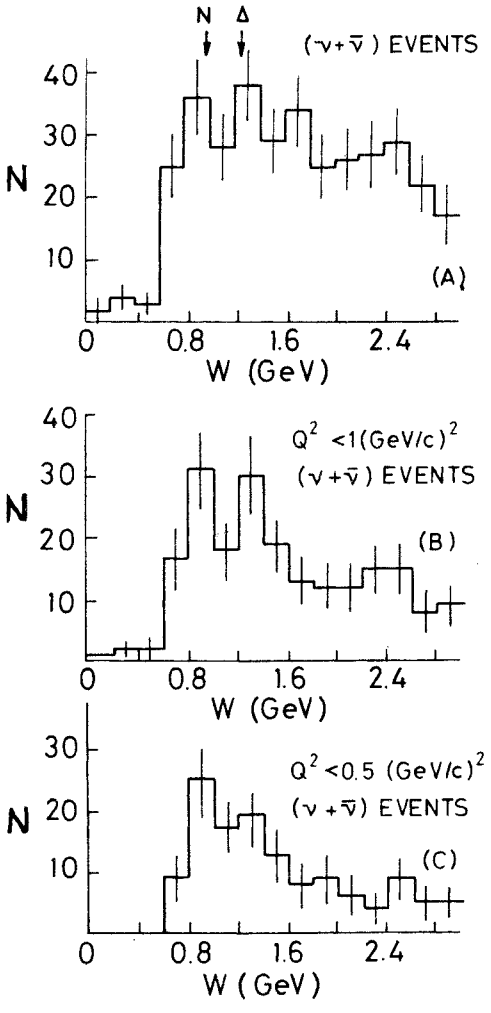

Fig. 1 Experimental distributions in invariant mass of the hadron system W for various cuts in Q^2.

In the neutrino energy interval 10 - 30 GeV there are 30 quasielastic and Δ events and 468.4 neutrino events corrected for detection efficiency. Normalizing to the cross section for the combined quasielastic and Δ production events, we obtain a value of $\alpha^\nu = (0.70 \pm 0.18) \times 10^{-38}$ cm^2/GeV. This value of α^ν is in good agreement with our previous measurement[1] and with the measurement of α^ν at lower energies [7]. The energy dependence of the total neutrino cross section was obtained by comparing the experimental energy distribution with the prediction of a monte carlo calculation using the method described in our previous work.[1] The resulting relative neutrino cross section is shown in Fig 2. It is seen that the cross section rise is consistent with a linear dependence on energy over the energy range of 10 - 240 GeV in agreement with the expectations of Bjorken scaling.[4] Using the absolute value of the cross section obtained at low energy from quasielastic and Δ production data an absolute cross section scale is obtained as shown in Fig 2. This scale has an uncertainty of approximately 20% due to the uncertainty in α^ν at low energy. Similarly the antineutrino relative cross section is obtained and reported in Fig 3. Again the data are consistent with a linear dependence on $E_{\bar{\nu}}$ up to $E_{\bar{\nu}} \sim 60$ GeV.

The ratio $\alpha^{\bar{\nu}}/\alpha^{\nu}$ was calculated using the quasielastic and Δ production events for both neutrino and antineutrinos and assuming the equality of these cross sections. From the sample of 30 antineutrino and 30 neutrino quasielastic and Δ production events we obtain a value of $\alpha^{\bar{\nu}}/\alpha^{\nu} = .41 \pm .11$ at a mean energy of 21 GeV, in agreement with our previous measurement (see Fig 4). It should be noted that although the statistical error on the value of $\alpha^{\bar{\nu}}/\alpha^{\nu}$ is large, the present measurement does not depend on the relative neutrino and antineutrino fluxes.

MEASUREMENT OF DISTRIBUTIONS IN THE SCALING VARIABLES x y and ν

The directly observed distributions in $x = Q^2/2ME_{\nu}$ for neutrinos and antineutrinos, combining data taken at 300 and 400 GeV, are plotted in Fig 5 for two different regions of neutrino and antineutrino energy. We show also the corresponding x-distributions calculated assuming scale invariance and the simplifying relations among the nucleon structure functions, viz: $2xF_1(x) = F_2(x)$, $xF_3(x) = -F_2(x)$, and $F_i(x) = \bar{F}_i(x)$, where $\bar{F}_i(x)$ refers to antineutrino-nucleon scattering. The form of $F_2(x)$ obtained from electroproduction experiments[5] (for $x \gtrsim 0.1$), the incident neutrino and antineutrino spectra[1] and the geometric detection efficiency of the apparatus[1,2] are included in obtaining the calculated distributions, which are normalized to the area of the experimental distributions. The x-distributions for neutrinos and antineutrinos are essentially the same, and are not significantly dependent on $E_{\nu}(E_{\bar{\nu}})$. In Fig 6 are plotted the y-distributions ($y = E_h/E_{\nu}$) for neutrinos and antineutrinos, and

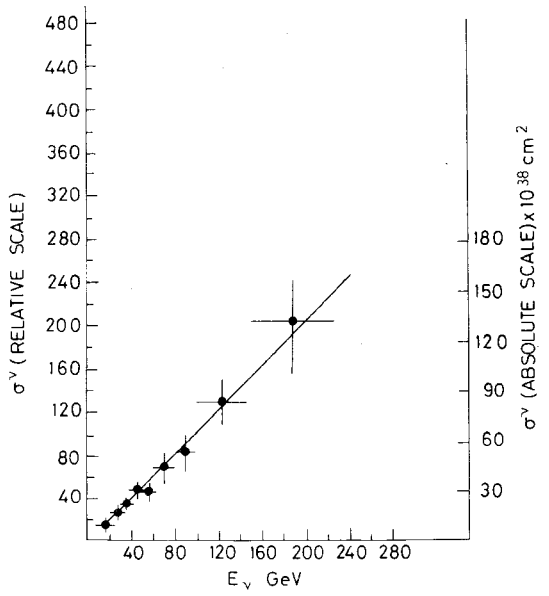

Fig. 2 Total cross-section as a function of neutrino energy.

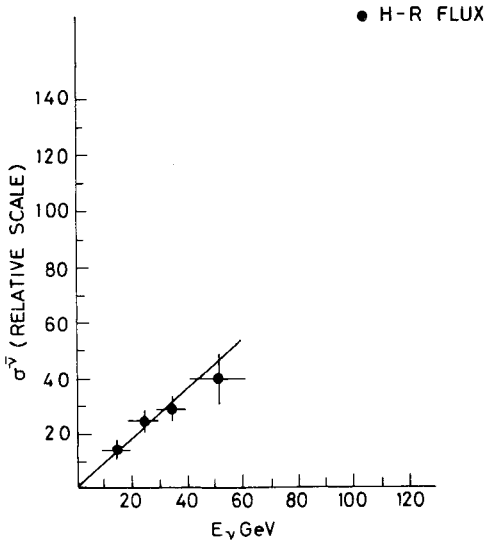

Fig. 3 Total cross-section as a function of antineutrino energy.

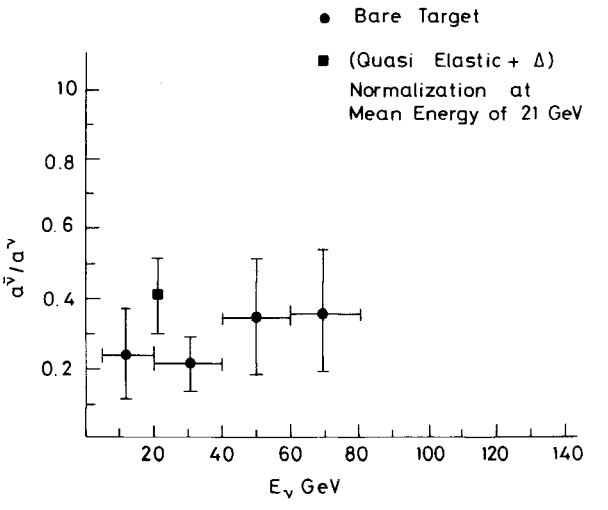

Fig. 4 Cross section ratio as a function of energy. Bare target measurements are from Reference 1.

the predictions that follow from scale invariance and assumptions described above. The y-distributions for neutrinos are consistent with these assumptions and with earlier data.[6] The y-distributions for antineutrinos, however, are not completely consistent with the simplest form expected from lower energy data[7], viz, $dN/dy \sim (1 - y)^2$.

A more general analysis of the y distribution may be made by relaxing the assumption that $xF_3(x) = -F_2(x)$. We can then write the scale invariant cross section for inelastic neutrino nucleon collisions in the form

$$\frac{d^2\sigma^{\nu,\bar{\nu}}}{dxdy} = \frac{G^2 ME_\nu}{\pi} F_2(x)\{1-y(1\mp B^{\nu,\bar{\nu}})+\frac{y^2}{2}(1\mp B^{\nu,\bar{\nu}})\}$$

where the upper (lower signs) are for neutrinos (antineutrinos), $B^\nu(x) = -xF_3(x)/F_2(x)$, and $B^{\bar{\nu}}(x) = -x\bar{F}_3(x)/\bar{F}_2(x)$.

Figure 7 shows the y distributions for two regions of x for neutrinos and antineutrinos. We have divided the data by the relative detection efficiency to display the corrected experimental distributions. For $x > 0.1$ it is seen that the excess of events at high y in the antineutrino distributions has largely disappeared. Note the difference in the antineutrino y distribution in the two x regions.

Also shown in Fig. 8 are the four values of $B^\nu(x)$ and $B^{\bar{\nu}}(x)$ obtained from the four y distributions of Fig. 7. Charge symmetry requires that $B^{\bar{\nu}}(x) = B^\nu(x) = B(x)$. In the region $x < 0.1$ the measured values of B^ν, $B^{\bar{\nu}}$ and $B(x)$ agree indicating that the data are consistent with charge symmetry. For $x < 0.1$ the measured value of $B^{\bar{\nu}}$ differes from the separately determined value of B^ν and $B(x)$ by about 3 standard deviations.

REFERENCES

1 A. Benvenuti et al., Phys. Rev. Letters 32, 125 (1974).

2 A. Benvenuti et al, Phys. Rev. Letters 32, 800 (1974); B. Aubert et al., Phys. Rev. Letters 32, 1454 (1974).

3 I. Budagov et al., Lettere Nuovo Cimento 2, 686 (1969); W. A. Mann et al., Proceedings of the XVI International Conference on High Energy Physics, Chicago-Batavia (1972); T. Eichten et al., Phys. Letters B46, 274 (1973); B46, 281 (1973); J. Campbell et al., Phys. Rev. Letters 30, 335 (1973). P. Schreiner and

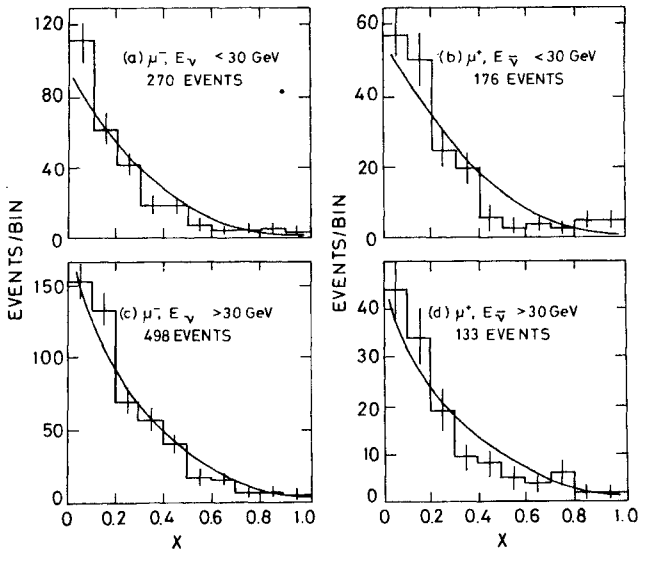

Fig. 5 Experimental distributions in $x = q^2/2ME_h$ and calculated distributions (solid lines) expected from scale invariance using $F_2(x)$ from electroproduction and simplifying relations among the structure functions (see text).

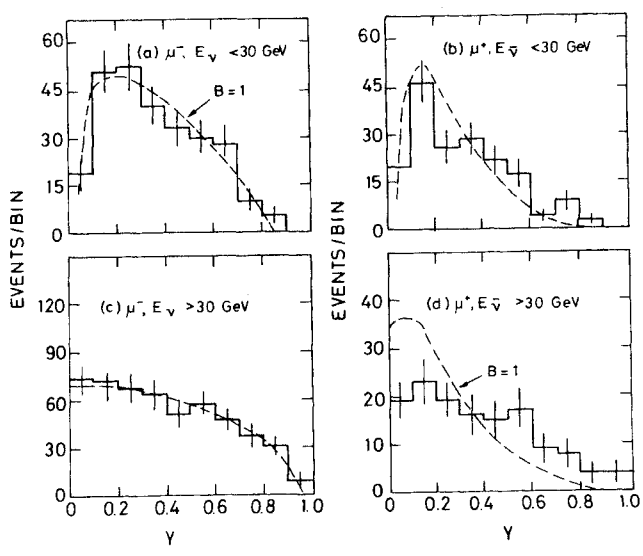

Fig. 6 Experimental and calculated distributions in $y = E_h/E_\nu$. The two curves are for $dN^\nu/dy = \text{const}$ and $dN^\nu/dy = (1-y)^2$. The fall off in the first y bin in (a) and (b) is due to the joint selection criteria $W^2 > 2.6\ GeV^2$ and $q^2 > 1.0\ GeV^2$.

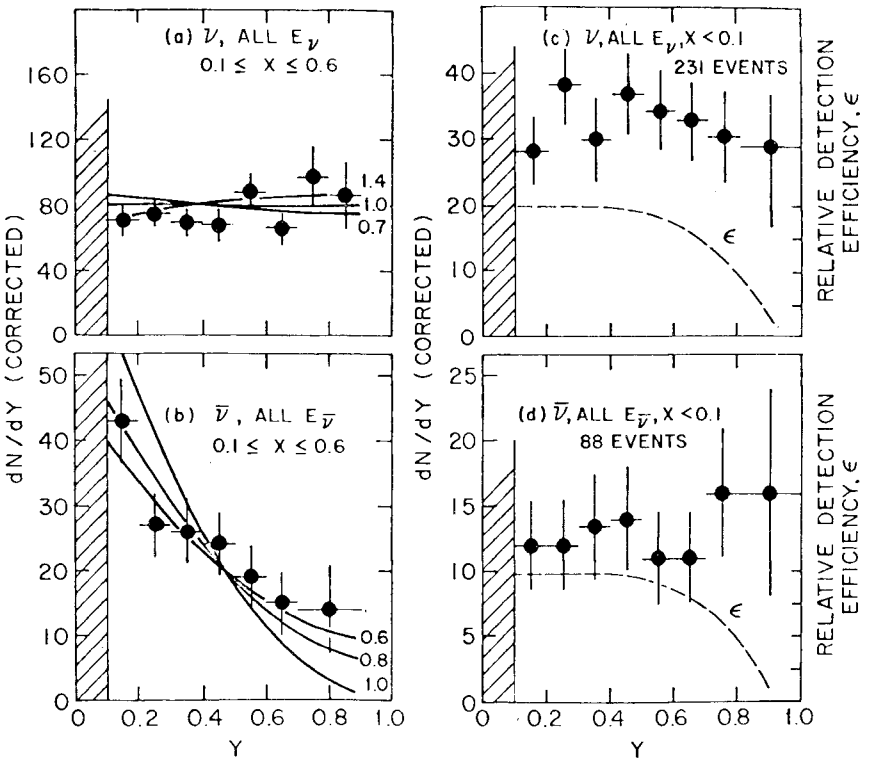

Fig. 7 Corrected experimental y-distributions for the region $0.6 > x \geq 0.1$ (a) and (b), and for the region $x < 0.1$ (c) and (d). Points at $y = 0.05$ are omitted because they are sensitive to resolution corrections. Points at $y = 0.95$ in (a) and (b) are omitted because they are sensitive to efficiency corrections. Calculated curves for different values of B^{ν} and $B^{\bar{\nu}}$ are also shown in (a) and (b).

reference 3 continued

F. Von Hippel, Phys. Rev. Letters 30, 339 (1973); P. Schreiner et al., Phys. Rev. Letters, 8, 339 (1973). M. Derrick, Quasielastic Neutrino Reactions: Form Factors, ANL Report 7350 (1973).

4 J. D. Bjorken, Phys. Rev. 179, 1547 (1969).

5 G. Miller et al, Phys. Rev. D5, 528 (1972).

6 B. C. Barish et al, Phys. Rev. Letters 31, 565 (1973).

7 D. H. Perkins, Proc. of the XVI International Conference on High Energy Physics, Chicago-Batavia 4, 189 (1972); T. Eichten et al , Physics Letters B46, 274 (1973); B46, 281 (1973).

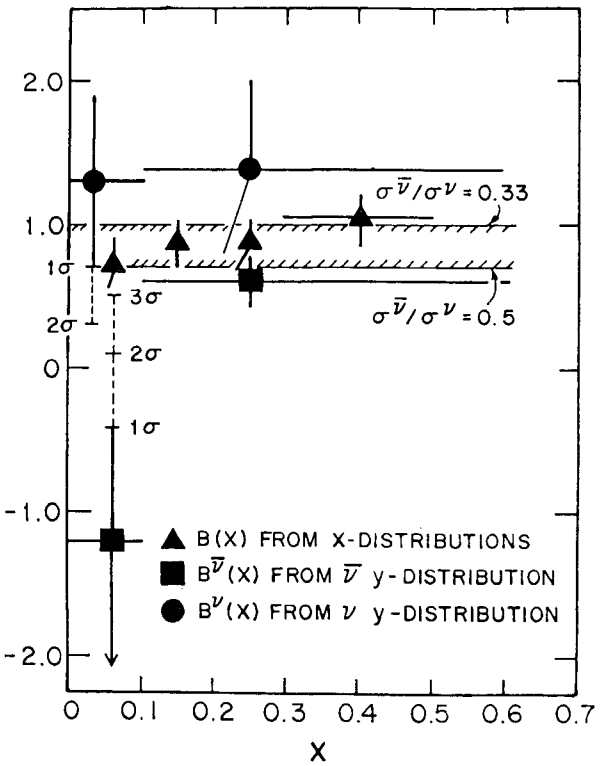

Fig. 8 Plot of the values of B(x), $B^{\nu}(x)$ and $B^{\bar{\nu}}(x)$ obtained from the experimental x- and y-distributions in the regions $x < 0.1$ and $0.6 > x \geq 0.1$. The three points in the $x < 0.1$ region, all of which should be plotted at $x = 0.05$, are shifted slightly with respect to each other for improved clarity.

CALTECH - FERMILAB EXPERIMENT

F Sciulli

California Institute of Technology

CALTECH - FERMILAB EXPERIMENT

This experiment was carried out in the FNAL dichromatic neutrino beam. Neutrinos interacting in a 170 ton iron target through the process

$$\nu_\mu + N \rightarrow \mu^- + \text{hadrons}$$

are selected when the muon traverses a trigger counter located downstream of the magnet. The muon and hadron energies (E_μ and E_h) are measured to the following accuracy:

E_μ: statistically 21%, systematically 5%

E_h: statistically 14-30% systematically 10%

The distribution in total observed energy ($E_{obs} = E_\mu + E_h$) is shown in figure 1. The characteristic two peak structure expected in a narrow band beam is clearly seen. The mean neutrino energies of the peaks are $\langle E\nu_\pi \rangle$ = 40 GeV and $\langle E\nu_K \rangle \approx$ 140 GeV.

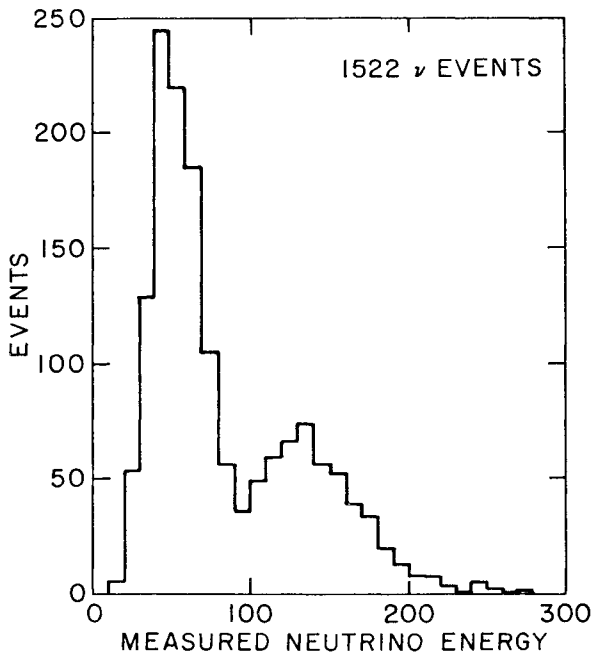

Fig. 1 Visible energy distribution showing two-peak structure characteristic of a narrow band beam.

1 DISTRIBUTION IN THE SCALING VARIABLE $x = Q^2/2ME_h$

Precise measurement of x-distributions require extremely good resolutions. Resolution effects change the shape of observed x-distributions as shown in Figure 2a. The curve labelled $F_2(x)$ is the structure function measured by SLAC-MIT with electrons on deuterium. When we fold in the experimental resolutions for this experiment, we find the expected experimental curve labelled $(F_2(x))_{smeared}$.

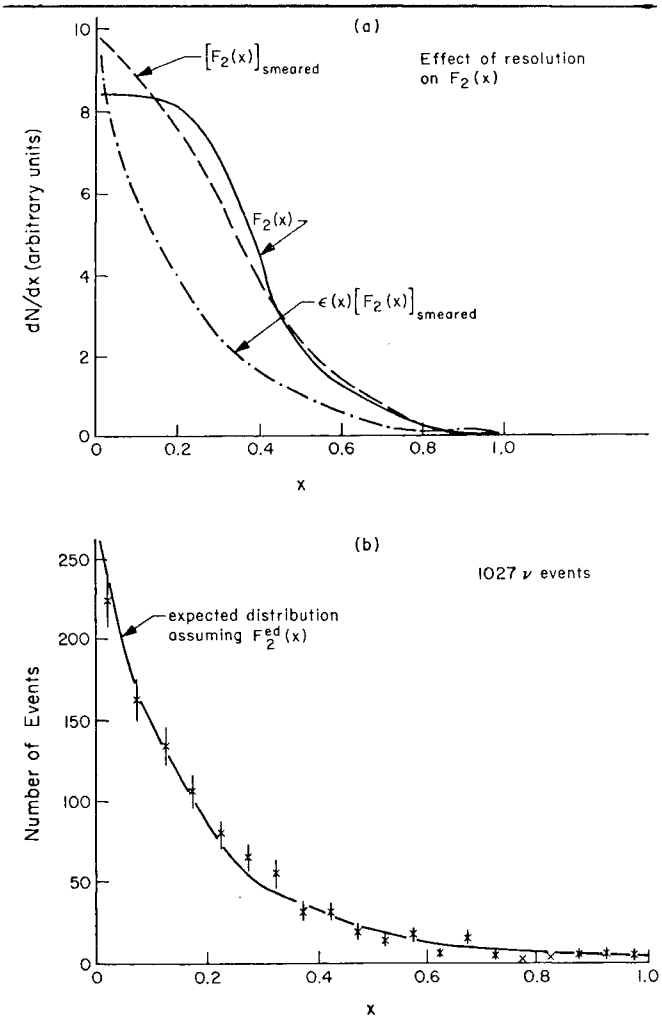

Fig. 2 Comparison of our data with the x distribution expected from electron-deuteron data after folding in our experimental resolution and acceptance.

If we further fold in the acceptance of the apparatus, we see the lower curve. Therefore, it should be emphasized that an $F_2(x)$ structure function of the same form as that obtained at SLAC will result in an experimental distribution that is sharply peaked near x = 0, and with a somewhat different falloff, coming from effects of resolution and acceptance. Figure 2b shows the observed x-distribution for the 1027 events inside our fiducual volume where both the muon and the hadron energies are measured. The solid curve is the expected distribution, assuming the SLAC $F_2^{ed}(x)$ structure function with resolutions and efficiencies folded in. There are no statistically significant differences observable between the x-distribution for pion neutrinos and kaon neutrinos.

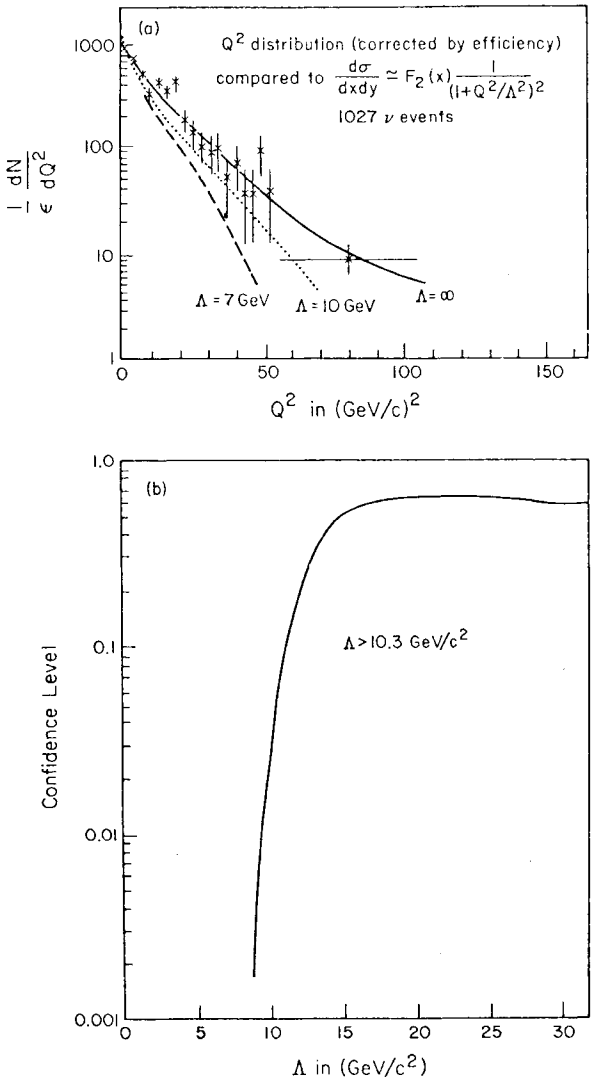

Fig. 3 Comparison of our q^2 distribution with expectations assuming $F_2^{ed}(x)$ from SLAC and a flat y distribution modified by a propagator factor, giving a lower limit to the mass term Λ.

2 TEST OF SCALING IN THE Q^2 DISTRIBUTION

The distribution in Q^2 corrected for efficiency, for all events is shown in the figure 3a. The expected distribution shown as the smooth curve, assumes the flat y-distribution as well as $F_2^{ed}(x)$ from SLAC. This curve is labelled $\Lambda = \infty$ in the figure. In order to test the sensitivity of the data to a possible breakdown of scaling or a propagator effect we have also included a multiplicative term $(1 + Q^2/\Lambda^2)^{-2}$, which modifies the expected behaviour giving a steeper falloff. For Λ = 10 GeV, for example, the calculated curve normalized to the data falls below the data at all points below the first. Figure 3b shows the confidence level for a fit to this propagator term. Above Λ = 15 GeV/c^2 we have no sensitivity; the fit is equally likely at $\Lambda = \infty$. Below 15 GeV/c^2, the likelihood falls rapidly. We place a 90% confidence on a propagator mass for the term we have included: $\Lambda > 10.3$ GeV/c^2.

3 DISTRIBUTIONS IN THE INELASTICITY VARIABLE $y = E_h/E_\nu$:

The y-distributions are more affected by the acceptance function than by resolution. The smooth curve shown in figure 4a is the expected y-distribution observed in our apparatus for ν interactions; effectively, it corresponds to the efficiency of the apparatus in the variable y. The data are shown on the same figure with the appropriate statistical error. Figure 4b shows the same distribution on a log scale. The systematically high points for y > 0.6 occur in a region where the efficiency has fallen below 10%. Below this value where the efficiency is high and well understood, there are no systematic departures from the expected flat distribution for neutrinos. We have chosen to

analyze our data for y < .6 only.

Figure 5a shows all the neutrino events with y < 0.6 corrected for efficiency and plotted vs. y. The data are consistent with the expected flat distribution. To obtain a numerical estimate of this consistency, we have fit to a function of the form

$$\frac{dN}{dy} = C\,(1 + a(1-y)^2) \qquad (1)$$

where C is constrained by the overall normalization, and a is a free parameter (it could be thought of as representing an average antiquark component in the nucleon). Figure 5 shows the result:

$$a = +0.05\ ^{+\ 0.25}_{-\ 0.17}$$

consistent with zero, and consistent with the 5% average anti-quark component found in the low energy CERN data.

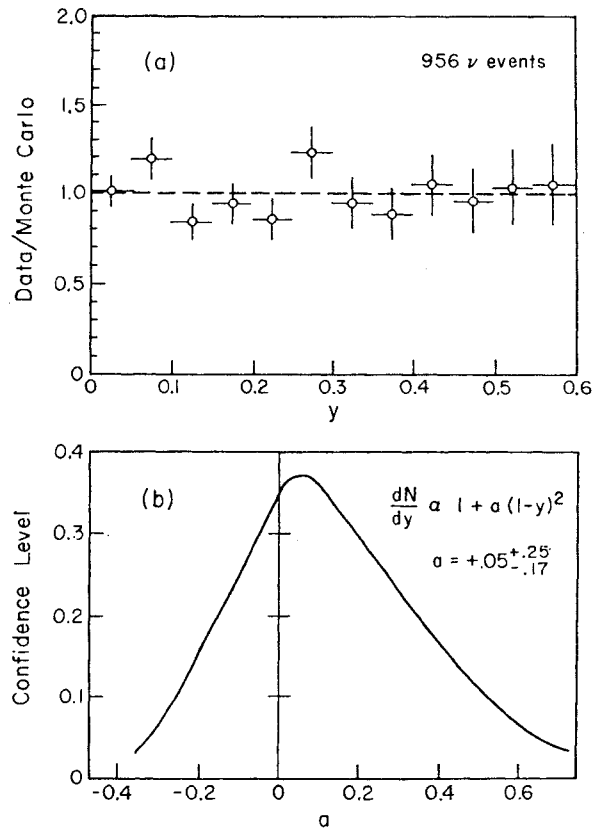

Fig. 5 Distribution in y for y<0.6 fitted to determine the average antiquark component in the nucleon.

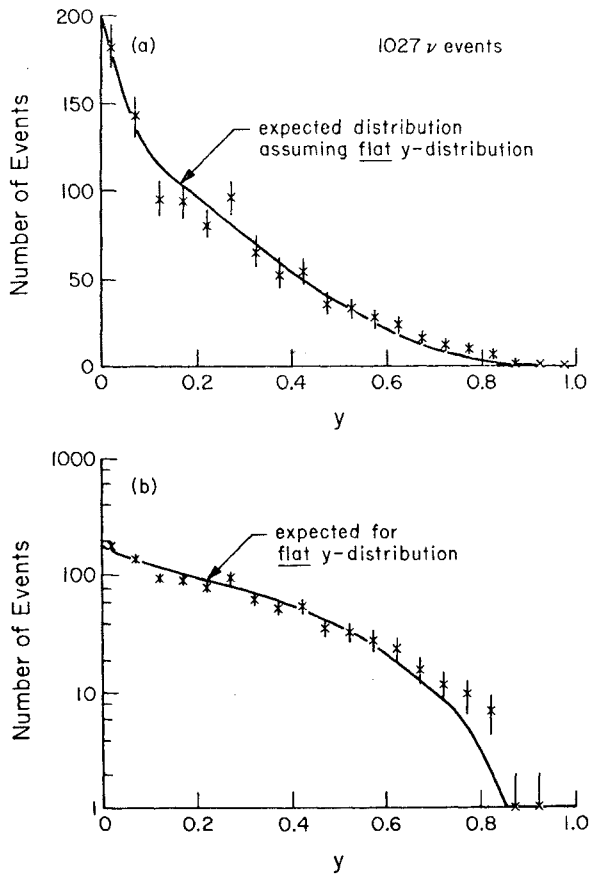

Fig. 4 Comparison of our data with a flat y distribution modified by our acceptance on (a) linear and (b) logarithmic scales.

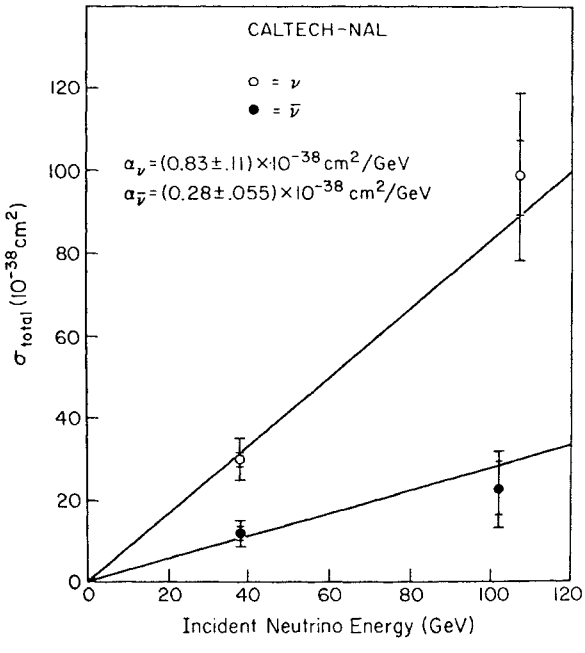

Fig. 6 Measured neutrino and antineutrino cross sections. The inner error bars represent the statistical errors and the outer ones the total errors.

4 NORMALIZED TOTAL CROSS SECTIONS

The cross-section has been measured in a separate run using the FNAL narrow band beam. This is the first measurement of σ_ν and $\sigma_{\bar{\nu}}$ at NAL energies in which the neutrino flux is measured directly in the same experiment. A more complete description of the experimental method used will be found in the paper submitted to the conference: (Paper 582; CALT-68-452.) Figure 6 shows the cross-sections measured in this experiment with statistical errors extending to the inner horizontal bars. The estimated systematic errors have been added in quadrature; the total errors are drawn to the outer horizontal bars. The best fits for α_ν and $\alpha_{\bar{\nu}}$ are

$$\alpha_\nu = (0.83 \pm 0.11) \times 10^{-38} \text{ cm}^2/\text{GeV} \quad (2)$$

$$\alpha_{\bar{\nu}} = (0.28 \pm .055) \times 10^{-38} \text{ cm}^2/\text{GeV} \quad (3)$$

The data points are quite consistent with this assumed linear relationship intersecting the origin.

Figure 7a shows the ratio of anti-neutrino to neutrino cross-sections at the two neutrino energies in this experiment. The ratio of slopes (equations (2) and (3)) is shown as the solid horizontal line. The sum of the slopes is shown in figure 7b, with the best fit line shown as well. For scattering dominantly from particle constituents of spin 1/2 (quarks) through V-A reaction, the ratio of $\sigma_{\bar{\nu}}/\sigma_\nu$ is equal to 1/3. The deviation from this value is a measure of the anti-quark component in the nucleon and/or breakdown of the Callan-Gross relation. Figure 8 shows the relative fraction of anti-quark ($\bar{Q}/Q$) and spin 0 (K/Q) component. The Callan-Gross relation would predict $K = 0$.

The slope ratio persists at high energy with a value close to 1/3. However, the higher energy experiments are still not able to determine the presence of anti-quarks at the 5% level.

In parton models, the sum of the slopes ($\alpha_\nu, \alpha_{\bar{\nu}}$) in neutrino and anti-neutrino scattering from nucleons

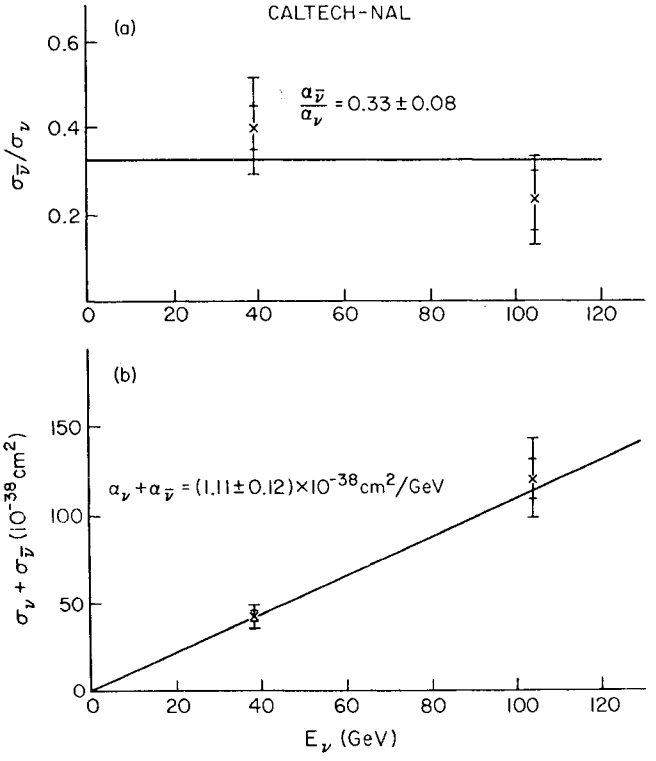

Fig. 7 Ratio and sum of the neutrino and antineutrino cross sections.

$$\sigma^\nu = \frac{G^2 s}{2\pi}\left[Q + \frac{1}{3}\bar{Q} + \frac{1}{2}K\right]$$

$$\sigma^{\bar{\nu}} = \frac{G^2 s}{2\pi}\left[\frac{1}{3}Q + \bar{Q} + \frac{1}{2}K\right]$$

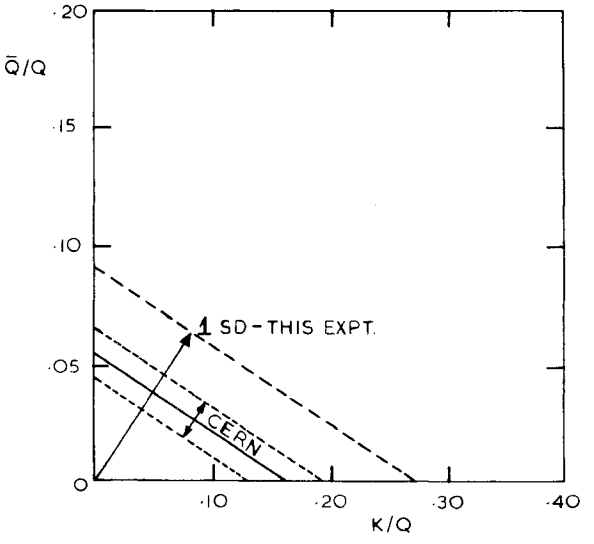

Fig. 8 One standard deviation limits imposed on the antiquark and spin - 0 components in the nucleon in this and the CERN experiments.

is related to the magnitude of the electro-magnetic scattering from nucleons through the mean-square charge of the constituents. This relationship may be expressed as follows

$$\langle q^2 \rangle = \frac{\int F_2^{\gamma N}(x)dx}{\frac{3\pi}{4G^2M}(\alpha_\nu + \alpha_{\bar{\nu}})} \qquad (6)$$

where $\langle q^2 \rangle$ is the mean square charge of the constituents in units of the electron charge, the numerator is the integral over the structure function, $F_2^{\gamma N}(x)$, measured in electron-deuteron deep inelastic scattering, with the contribution from strange quarks subtracted. We have taken here

$$\int F_2^{\gamma N}(x)dx = 0.15 \pm .02$$

For scattering from constituents that have fractional charge (eg quarks), or fractional effective charge (eg Han-Nambu quarks below colour threshold), one expects relatively small values for $\langle q^2 \rangle$. For example, the simplest quark model would give $\langle q^2 \rangle = 5/18 = .28$. Integral charges for the constituents,[10] on the other hand, require $\langle q^2 \rangle \geq 0.5$. We see from figure 9 that the relatively small value for $\langle q^2 \rangle$ continues at 38 and 105 GeV. Averaging the data from this experiment, we obtain for $E_\nu > 30$ GeV

$$\langle q^2 \rangle = .27 \pm .05$$

in agreement with that expected for scattering from quarks.

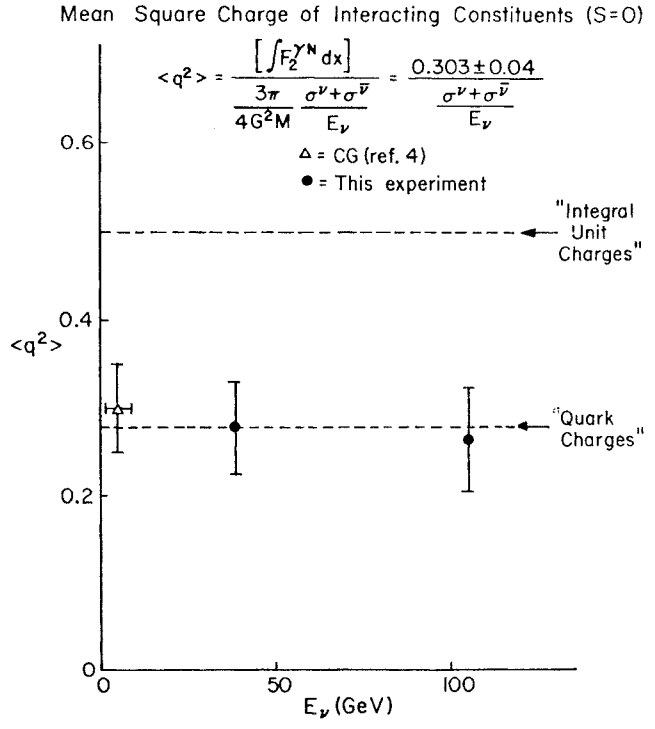

Fig. 9 Mean square charge of the nucleon constituents derived from $\int F_2^{\gamma N}$ and the sum of neutrino and anti-neutrino cross sections.